PFG 2013 / 1, 005–0017 **Article**
Stuttgart, February 2013

Neural Network Modelling of Tehran Land Subsidence Measured by Persistent Scatterer Interferometry

Maryam Dehghani, Shiraz, Iran, Mohammad Javad Valadan Zoej & Iman Entezam, Tehran, Iran

Keywords: persistent scatterer, neural network, modelling, sensitivity analysis

Summary: A large area located in the southwest of Tehran is subject to land subsidence induced by over-exploitation of groundwater. Since the use of conventional SAR Interferometry was not possible due to the large spatial baseline and rapid temporal decorrelation, persistent scatterer interferometry (PS-InSAR) using two different ascending and descending datasets of ENVISAT ASAR was applied in order to monitor the deformation. PS-InSAR is a recently developed technique used to address the decorrelation problem by identifying scatterers, called persistent scatterers (PS), the echo of which varies little in time. The estimation of the deformation rate was thus possible only in the PS pixels. In order to retrieve the spatial pattern of the subsidence, deformation rate at non-PS pixels were estimated by a proposed neural network modelling method separately applied on both descending and ascending datasets. Input variables of the network are geology and hydrogeology parameters of the aquifer system, while the network output is the subsidence rate. The performance of the neural network trained by the PS pixels was tested on a separate validation data. It was found that the trained network is able to predict the subsidence rate with the accuracy of less than 5 mm/a. The results were then compared to the levelling measurements acquired over a different time interval. The root-mean-square error (RMSE) between the measurements and the modelled deformation rate across the leveling tracks is 19.8 mm/a. The different deformation rates of both datasets in some points were most likely due to the different time intervals covered by the radar and levelling data. Neural network-based sensitivity analysis was finally performed to evaluate the influences of different geology and hydrogeology factors on the subsidence. The sensitivity analysis results that were interestingly similar for both radar datasets showed that the hydraulic conductivity, the thickness of fine-grained sediments and the water level decline are the first three most effective factors on the subsidence occurrence in Tehran basin.

Zusammenfassung: *Neuronales Netz zur Modellierung von Bodensenkungen bei Teheran gemessen durch Persistent Scatterer Interferometry.* Ein großes Gebiet südwestlich von Teheran ist von Bodensenkungen wegen übermäßiger Grundwasserentnahme betroffen. Die vorliegende Untersuchung baut auf zwei Datensätzen von ENVISAT ASAR auf, einem in Nord- und einem in Südrichtung geflogenen. Früher war der Einsatz von SAR Interferometrie wegen langer Basen und zu schneller zeitlicher Veränderungen am Objekt nicht möglich. Die neue Persistent Scatterer Methode (PS-InSAR) nutzt Objekte, deren Reflexionscharakteristik nur einer geringen zeitlichen Variabilität unterliegt. Allerdings kann die Deformation nur an ausgewählten, den so genannten PS-Pixeln bestimmt werden. Die dazwischenliegenden Räume wurden in dieser Untersuchung durch neuronale Netze überbrückt, die geologische und hydrogeologische Parameter berücksichtigen. Die innere Genauigkeit der Methode wurde durch unterschiedliche Trainingsdatensätze überprüft und ergab eine Genauigkeit der Prognose des Senkungsbetrages von weniger als 5 mm/a. Die äußere Genauigkeit wurde durch Nivellement bestimmt und ergab einen RMS-Fehler entlang der Nivellementslinien von 19,8 mm/a. Die große Abweichung dürfte auf unterschiedliche Zeitintervalle zwischen der SAR-Datenerfassung und den Nivellements beruhen. Die neuronalen Netze wurden außerdem zur Bewertung des Einflusses von geologischen und hydrogeologischen Parametern auf die Senkungsraten eingesetzt. Als die drei wichtigsten Einflussfaktoren haben sich die hydraulische Leitfähigkeit des Untergrundes, die Mächtigkeit der feinkörnigen Sedimente und der Rückgang des Grundwasserspiegels gezeigt. Beide SAR-Datensätze führten zum gleichen Ergebnis.

DOI: 10.1127/1432-8364/2013/0154 1432-8364/13/0154 $ 3.25

1 Introduction

Excessive groundwater pumping causes an increasing effective stress in aquifer systems. The changes in the effective stress cause some degree of compaction in fine-grained sediments within the aquifer system resulting in land subsidence. The land subsidence induced by overexploitation of groundwater is one of the major problems with its environmental consequences in most parts of Iran. One of these areas is located in the southwest of Tehran, the capital city of Iran. The Tehran Basin with an area of 2250 km^2 is located between the Alborz Mountains to the north and Arad and Fashapouye Mountains to the south.

The National Cartographic Center (NCC) of Iran firstly measured the land subsidence by precision levelling during 1995–2002. Later, the Geological Survey of Iran (GSI) in cooperation with other organizations including NCC and the Water Management Organization launched a comprehensive study on subsidence in and around Tehran. The area was studied from different points of view including geology, geophysics, tectonic and geotechnics. According to the geological map (1:100,000 scale), the Tehran Basin consists of different geological units including lower-middle Eocene (Karaj formation) and Quaternary units. The southern part of the area primarily contains Quaternary (Qt1 and Qt2) units as indicated in Fig. 1b. The Qt1, or Kahrizak formation, features different properties in the northern and southern parts of the area, consists of silt and cream clay in the subsidence area, and is exposed by different faults such as the Kahrizak, south Rey and North Rey faults (Fig. 1a). The deposit of fine-grained sediments due to flooding generates the clay silt of Kahrizak. The Qt2, or Tehran formation, contains young alluvial fans mainly covering the southern part of the Tehran Basin. This formation has an unsorted alluvial and a flood deposit with an average thickness of 60 m, primarily composed of gravel, pebble and sand in a sandy silt matrix (Shemshaki et al. 2005).

The extent and thickness of the fine-grained sediments serves as one of the most important factors for land subsidence caused by groundwater extraction. The greater extent and thickness an aquifer system has, the more compaction occurs. According to the studies performed by the Engineering Geology group of the Geological Survey of Iran (GSI), the thickest part of the alluvial layers that constitute the aquifer system belongs to the area with a higher subsidence rate. The contours indicating the alluvial thickness are illustrated in Fig. 4e. Moreover, the central part of the subsidence

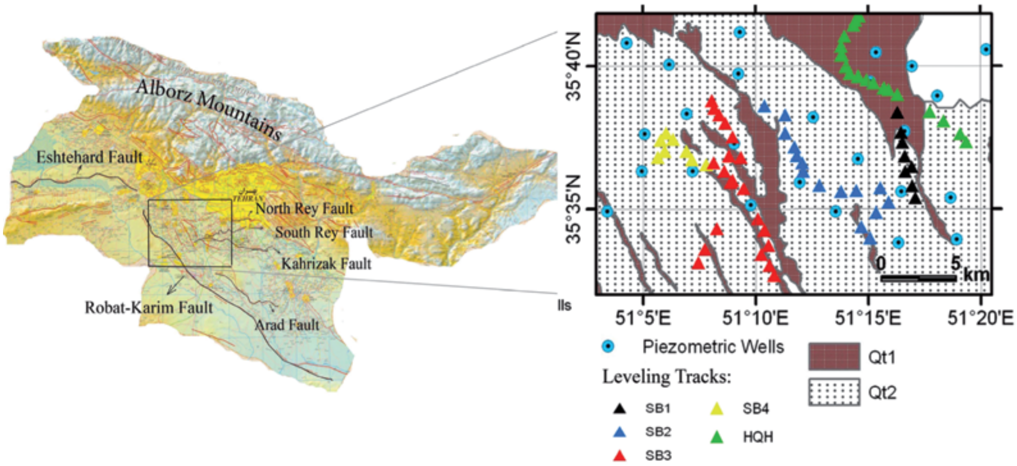

(a) (b)

Fig. 1: (a) Location of different faults surrounding the study area in Tehran province. The black rectangle depicts the area subject to subsidence. (b) Geological units mainly consisting of Quaternary sediments. The blue circles represent piezometric wells while the black triangles indicate the levelling stations.

area contains higher amounts of fine-grained sediments, including clay, at up to 100% as observed in Fig. 4f. Moreover, geotechnical tests indicate that the storage coefficient have smaller values in the southern part of the aquifer system compared to the northern part (Fig. 4c). The decrease of the storage coefficient is due to the existence of higher amounts of fine-grained sediments in the aquifer system. The average value of the storage coefficient of Tehran aquifer system is estimated as 5% (Shemshaki et al. 2005). Moreover, as shown in Fig. 4d, the hydraulic conductivity of the aquifer system decreases generally from north to south of the area and in the northeast of the area. The decrease of the hydraulic conductivity in the northeast is mostly due to the decrease of thickness of the saturated zone.

The main part of the Tehran basin dedicated to the agricultural activities is subject to the land subsidence due to the over-exploitation of groundwater. According to the latest studies, groundwater level depth exceeds 100 m in the north of the aquifer system (Fig. 4b). A unit hydrograph of the Tehran basin (Fig. 2) indicating the overall changes of water level was extracted from the piezometric information (Shemshaki et al. 2005). The locations of piezometric wells are shown in Fig. 1b. As observed in Fig. 2, the water level dramatically declined by about 9 m in 20 years. The volume change of the aquifer system during 10 years is estimated as 6.6 km^3. The number of pumping wells has increased from 3906 in 1969 to 26076 in 2003. A comparison of the number of wells and the volume of the extracted water between 1968 and 2003 shows that the ability of the aquifer system to yield water has significantly decreased due to insufficient recharge. The water level changes between 1968 and 2003 are shown as contour lines in Fig. 4a.

Among the various ground- and space-based techniques available, interferometric Synthetic Aperture Radar (InSAR) provides precise measurements of land surface deformation over large areas and at high spatial resolution (Galloway et al. 1998, Amelung et al. 1999, Peltzer et al. 1998, Fruneau & Sarti 2000, Tesauro et al. 2000, Crosetto et al. 2002, Motagh et al. 2006). However, conventional interferometry fails when the ground surface is covered by significant amounts of vegetation, due to a loss of correlation (Galloway & Hoffmann 2007) as in Tehran basin. Persistent scatterer InSAR (PS-InSAR) is a recently developed technique used to address the decorrelation problem by identifying scatterers, called persistent scatterers (PS), the echo of which varies little in time (Ferretti et al. 2000, Hooper et al. 2004, Kampes 2005). PS-InSAR gives measurements at a few sparse locations, i.e. PS points. However, despite of the improvement due to PS-InSAR approaches it should be noted that, if the spatial density of the detected persistent scatterers is low, the deformation pattern cannot be reliably retrieved. A sufficient number of PS pixels is required to map local variation of the deformation for deeper understanding of the subsidence extent and spatial distribution that enables us to better manage the water resources and construction tasks. It is however impor-

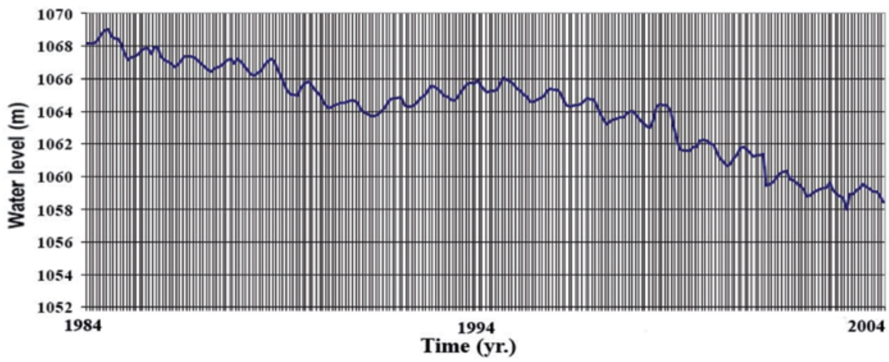

Fig. 2: Unit hydrograph for the Tehran aquifer system extracted from the groundwater information (Shemshaki et al. 2005).

tant to have the subsidence spatial extent and pattern for land managements (González & Fernández 2011). As in the Tehran basin many agricultural fields exist, the persistent scatterer density is low due to the lack of coherent scatterers over the time interval of consideration. There are various algorithms to retrieve the spatial pattern of the subsidence using the values at PS pixels. Classic interpolation techniques such as kriging can be generally used to estimate the deformation at a non-persistent scatterer based on the known deformation of surrounding persistent scatterers. However, these methods are based only on the deformation values of the neighbouring pixels. There are some analytical methods that try to predict the aquifer compaction using the geology and hydrogeology information (Hoffmann et al. 2003). However, we are left with great errors using these methods when we are facing the lack of accurate and detailed information of the aquifer system.

In such cases, the methods based on the intelligence systems can be effectively used instead of modelling the subsidence. In this paper we present a method based on a backpropagation neural network in order to model the subsidence signal. The deformation at non-persistent scatterer is estimated by neural network interpolation using not only the PS-InSAR derived deformation of the persistent scatterers but also their hydrogeology properties that highly affects the subsidence. The constructed neural network is trained using the hydrogeology parameters of the aquifer system as input variables of the network and PS-InSAR derived subsidence rate at PS pixels as the network output. The PS pixels whose deformation could be measured by PS-InSAR are used to train the network. The trained neural network is then used: (i) to retrieve the spatial pattern of the subsidence or to estimate the subsidence rate at non-PS pixels and to (ii) perform sensitivity analysis to identify a hydrogeology factor with the most influence on the subsidence. In other words, we can recognize to which hydrogeology factor the subsidence in Tehran basin is most sensitive.

This paper is structured as follows: Section 2 presents the proposed modelling method based on neural network and the mathematical framework of the sensitivity analysis. In section 3, the information layers fed to the neural network and the obtained results will be presented. Moreover, the sensitivity analysis results are given in this section. Finally, concluding remarks are given in section 4.

2 Subsidence Modelling based on Neural Network

Neural networks are based on the structure and functioning of the human brain and consist of a large number of simple processing units known as neurons. The neural network function is determined largely by the connections between neurons. It is trained by adjusting the values of the connections (weights) between neurons so that a particular input leads to a specific target output. The network is adjusted based on a comparison of the output and the target until the network output matches the target.

The output signal of neuron k in layer l is calculated as follows:

$$\begin{aligned} y^{(l)}{}_k &= s^{(l)}{}_0\,(w^{(l-1)}{}_{k1} \cdot y^{(l-1)}{}_1 + \ldots \\ &\qquad + w^{(l-1)}{}_{kK_{l-1}} \cdot y^{(l-1)}{}_{K_{l-1}} + w^{(l-1)}{}_{k0}) \\ &\qquad 1 \le k \le K_l \end{aligned} \tag{1}$$

Where K_l is the number of neurons in layer l, $s^{(l)}{}_0\,(.)$ is the activation function, $w^{(l-1)}{}_{ki}$ is the weight of the input $y^{(l-1)}{}_{ki}$ to the neuron k in which $1 \le i \le K_{l-1}$ and $w^{(0)}{}_{k0}$ is the bias value corresponding to the neuron k. It should be noted that $y^{(l-1)}{}_{ki}$ is actually the output of ith neuron in the previous layer. If $l = 1$, $y^{(l-1)}{}_{ki}$ is the input variables to the neural network. Weights are updated using the mean-squared error (MSE) as cost or error function through the training process. Readers are referred to e.g. Haykin et al. (1995) for further information about the training process and updating the weights.

One of the important factors that affect the success of modelling procedure is the ability to extract information about the relationships between the model structure's inputs and outputs from the trained neural network (Hashem 1992). This information can be used as a basis for the analysis of the model and determination of the most significant factors that affect it. HASHEM (1992) presented a closed-form expression for first order as well as higher order output sensitivities w.r.t. variations in the input variables for multilayer feedforward neural networks. These sensitivities can be used as a basis for inference about input-output relationships. In order to estimate the sensitivity of the network output w.r.t. to its inputs, the partial derivative, $\frac{\partial y}{\partial x_i}$ is estimated where y is the network output and x_i is its ith input. Consider a neural network with 2 hidden layers consisting of K_1 and K_2 neurons. $\frac{\partial y}{\partial x_i}$ is then calculated as follows:

$$\frac{\partial \hat{y}}{\partial x_i} = \sum_{k_2=1}^{K_2} \frac{\partial \hat{y}}{\partial y^{(2)_{k_2}}} . \frac{\partial y^{(2)_{k_2}}}{\partial y^{(1)}} . \frac{\partial y^{(1)}}{\partial x_i} \quad i = 1,...,n \quad (2)$$

Where n is the number of input variables, $\hat{y}$ is the network output, and $y^{(1)}$ and $y^{(2)}$ are the outputs of the first and second hidden layer, respectively. x_i is its ith input. The updated weights from training step are used to calculate (2). The more sensitive the output w.r.t. to x_i is, the higher the $\frac{\partial y}{\partial x_i}$ is. A little change to x_i will then cause a great change to the output $\hat{y}$.

Subsidence due to the over-exploitation of groundwater is a complex procedure influenced by different geology and hydrogeology factors. Groundwater information collected at different piezometric wells in the Tehran basin showed that the water level decline is not the only important cause for the subsidence occurrence in this area (DEHGHANI et al. 2010). Instead, some other geology and hydrogeology factors such as the fine-grained sediments thickness in the aquifer system are controlling the subsidence rate. In this paper, a method based on neural network is presented to model the subsidence for areas in which we could not measure the deformation rate using PS-InSAR. Moreover, in order to identify the main

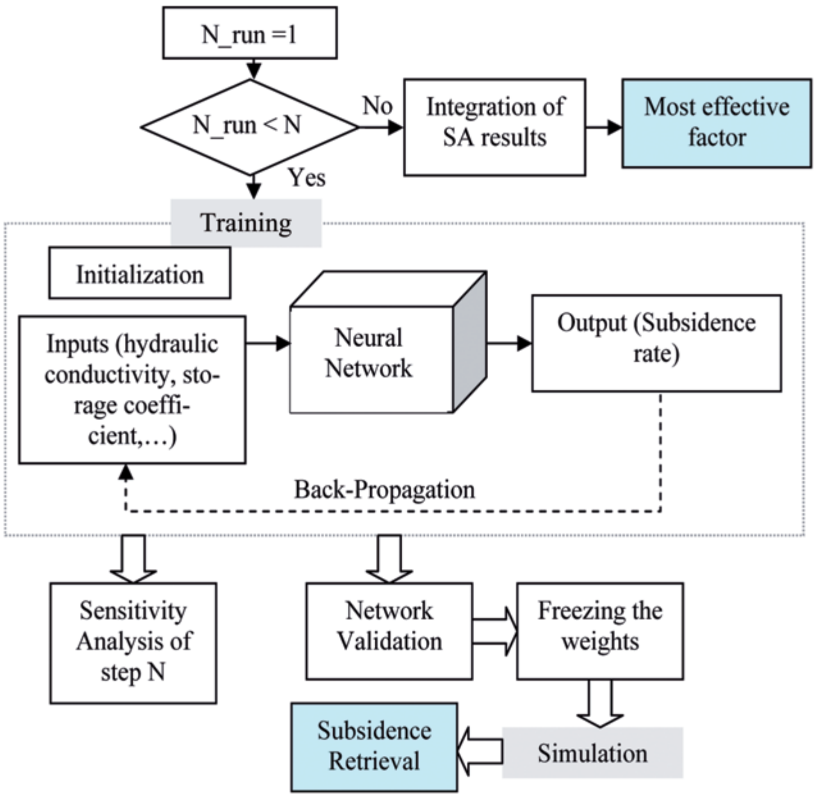

Fig. 3: Framework of the presented method for modelling the subsidence and sensitivity analysis.

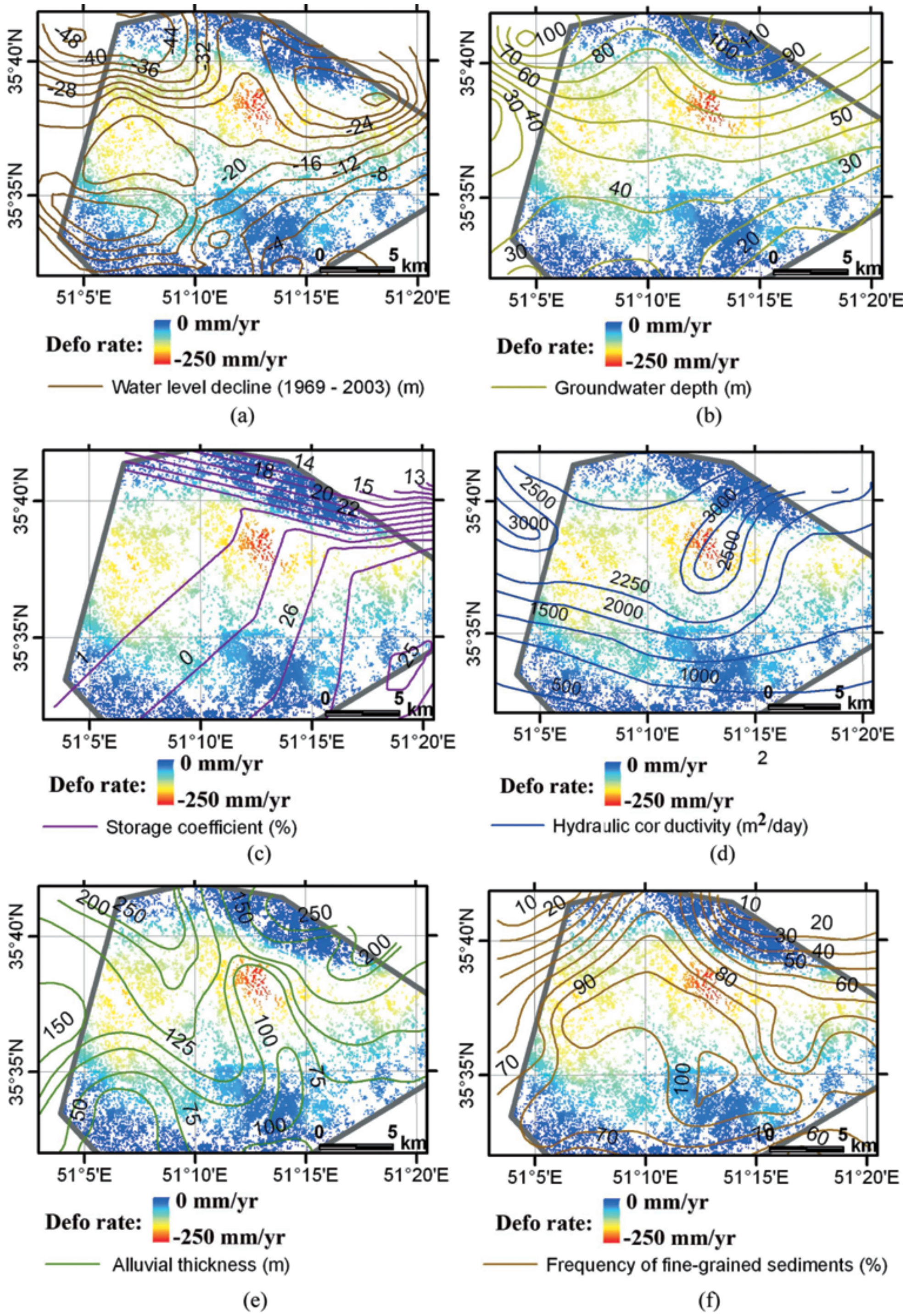

Fig. 4: Network inputs and output: (a) water level decline between 1969 and 2003, (b) groundwater depth, (c) storage coefficient, (d) hydraulic conductivity, (e) alluvial thickness, (f) frequency of fine-grained sediments in terms of percentage.

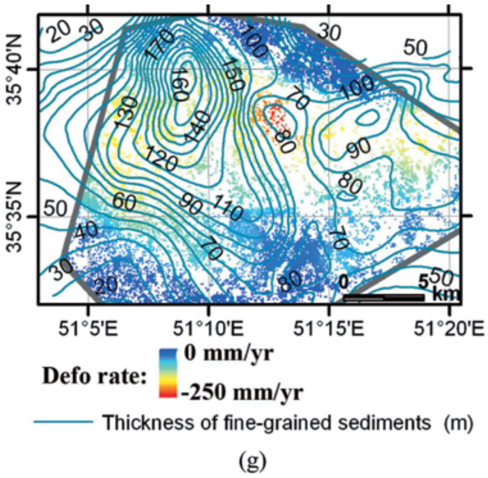

Fig. 4: Network inputs and output: (g) thickness of fine-grained sediments.

controlling factors in the Tehran basin subsidence, the sensitivity analysis was performed using the trained network. The framework of the presented method for subsidence modelling and sensitivity analysis is illustrated in Fig. 3.

The first step in the network construction is to determine the number of layers and their neurons as well as the activation functions. The most proper network architecture here was identified in a trial-and-error manner. As the network initialization for training is randomly done, the obtained results including the updated weights and the sensitivity analysis result are slightly different in each run. It should be noted that each run includes a complete training procedure. The criterion for stopping the training procedure in each run is the number of iterations. According to Fig. 3 a neural network is fully trained in N independent runs where N can be arbitrarily set. The trained network is tested at the end of each run using the validation data. Moreover, the sensitivity analysis result obtained in each run will be saved for further integration. The updated weights corresponding to the minimum overall network error are used for the final simulation step.

The network input variables are hydrogeology factors controlling the subsidence rate while the output is the subsidence rate at PS pixels derived from PS-InSAR. The Tehran basin subsidence was monitored using PS-InSAR technique by which the annual deformation rate was measured at persistent scatterer locations. The available radar data consisted of 22 descending ENVISAT ASAR images of track 149 acquired between 2003 and 2008 and 19 ascending ENVISAT ASAR images of track 414 spanning between 2004 and 2009. PS-InSAR method was separately applied on both ascending and descending radar data. The results obtained from PS-InSAR indicate that the deformation time series contained a significant linear component on which the insignificant seasonal fluctuations are superimposed (Dehghani et al. 2010, Dehghani et al. 2009). The PS-InSAR results were then used to extract the annual deformation rate that is assumed to be constant from 2003 to 2009 as deformation time series suggested. The estimated subsidence rates obtained from descending and ascending data are slightly different due to the different imaging geometries of both datasets and non pure vertical components of the deformation system (Samieie-Esfahany et al. 2009).

The number of PS pixels detected from ascending and descending data is around 400,000 and 800,000, respectively. Due to the low spatial density of PS pixels, the deformation pattern cannot be easily recognized in the area. Hence, the presented modelling method is used to estimate the deformation rate at non-persistent scatterers in order to retrieve the deformation pattern. About 60% of the detected persistent scatterers are used to train the network while the rest is applied for network validation. The introduction of the inputs and output of the network as well as the obtained results from the modelling are presented in the next section.

3 Results

The available hydrogeology information of the Tehran basin includes hydraulic conductivity, storage coefficient, frequency and thickness of fine-grained sediments, groundwater depth, amount of water level decline between 1969 and 2003 extracted from piezometric measurements and alluvial thickness of the Tehran aquifer system. These properties were measured at different measurement sites across the study area using various methods including geotechnical testing and geophysics approaches. The point measurements were then converted to contour lines using interpolation. All the information layers superimposed as contours on the deformation rate map of PS pixels are shown in Fig. 4 as already explained.

In order to make the hydrogeology data compatible with the PS-InSAR-derived subsidence data in the neural network, all data were interpolated into grids with the pixel size of 90 m. Therefore, the total number of 320 × 210 pixels for which there are 7 features, i.e. hydrogeology information, covered the study area. A network consisting of two hidden layers of 20 and 5 neurons with the tangent sigmoid activation function was constructed. The hydrogeology information at PS pixels and their derived deformation rate were used as the network input and output, respectively. The constructed network was trained using 60% of the detected PS pixels. As already noted, the network was constructed in *N* runs (*N* is here set to 50) for each of which the trained network was tested using the validation data, i.e. 40% of the PS pixels. After comparing the results of different runs, the weights corresponding to the minimum overall network error are used for final simulation step.

The correlation between the trained network output and the observed subsidence rate for training and validation pixels in both ascending and descending datasets is illustrated in Fig. 5.

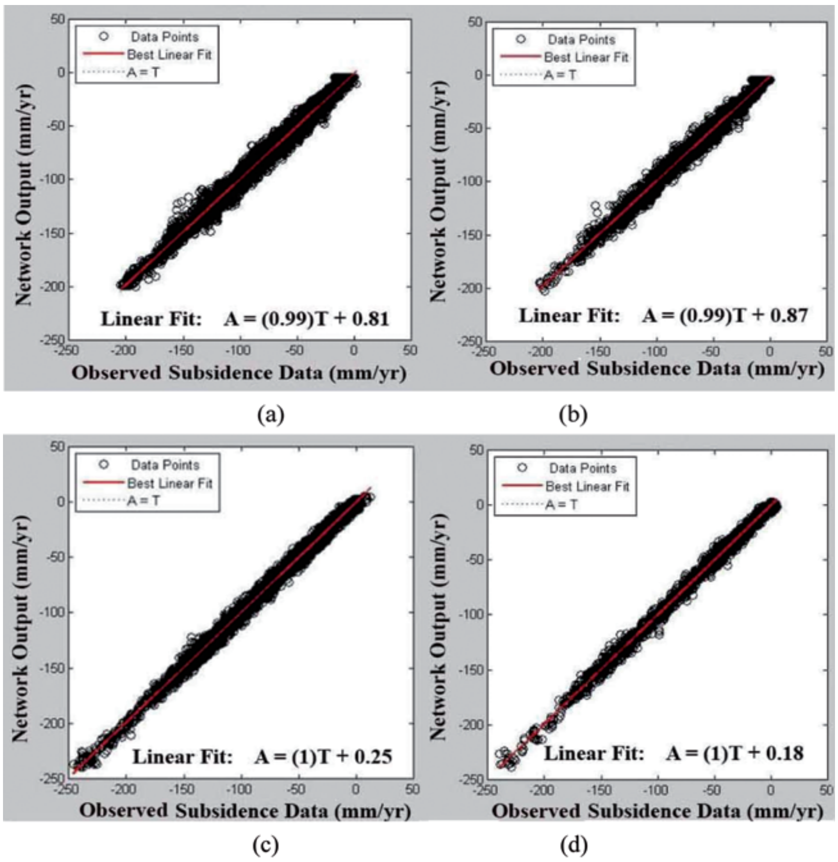

Fig. 5: Correlation between the subsidence rate simulated from the trained network (y axis) and the observed one derived from the PS-InSAR (x axis) for different datasets: (a-b) training and validation data of the descending mode, and (c-d) training and validation data of the ascending mode.

As can be observed in Fig. 5, a high correlation exits between the simulated subsidence data and the observed one extracted from PS-InSAR. The linear regression equation for each dataset presented below its corresponding plot is significantly close to A=T where A and T is the simulated and observed deformation values, respectively. In order to better validate the performance of the model, the subsidence rate at all PS pixels (training and validation pixels) for which the observed subsidence rate is available from PS-InSAR is simulated by the trained network as shown in Fig. 6. In this figure, the observed and simulated subsidence rates for both datasets are illustrated. Furthermore, the residual map as the

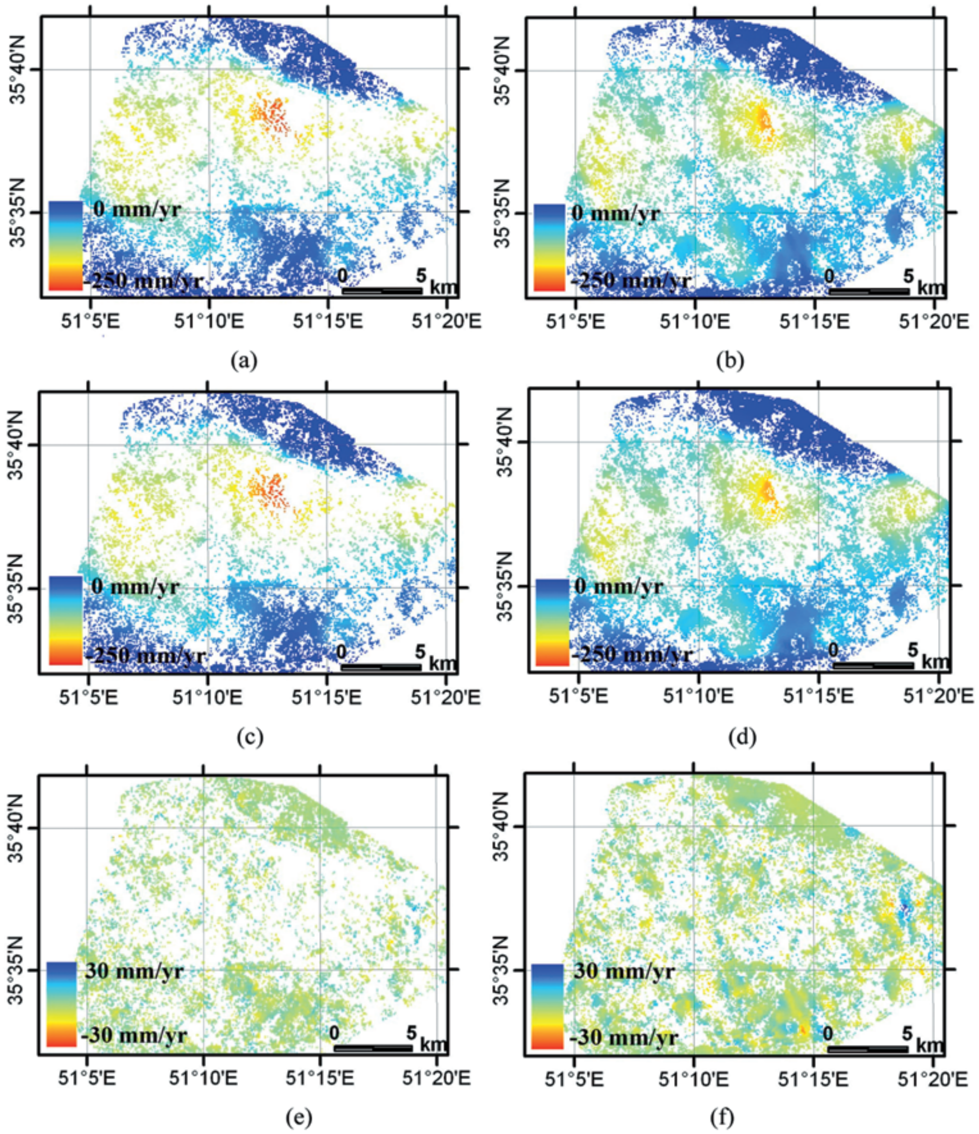

Fig. 6: Observed deformation rate obtained from the (a) descending and (b) ascending data; simulated deformation rate using the (c) descending and (d) ascending data; residual map as the difference between the observed deformation rate and the simulated one using the (e) descending and (f) ascending data.

difference between the observed and modelled subsidence rate is presented in Figs. 6c and 6f. Accordingly, the most amount of subsidence could be simulated by the proposed model and the residual map has a noisy behaviour rather than a systematic one. The root-mean-square error (RMSE) of the residual map is estimated as 3.53 mm and 4.58 mm for the descending and ascending datasets, respectively. The low values of RMSE are an indication of the high performance for the subsidence modelling.

The subsidence rate for all pixels (PS and non-PS) in the study area was then simulated by the trained network (Fig. 7).

As shown in Fig. 7, the spatial subsidence pattern including 3 main lobes has been retrieved. The slight difference observed between the spatial subsidence patterns simulated from descending and ascending modes is related to their different imaging geometry. The maximum deformation rates estimated from descending and ascending datasets are 241 mm/a and 203 mm/a, respectively. The coincidence of the spatial pattern of the subsidence area with the cultivated area indicates that the subsidence in the Tehran basin is due to groundwater exploitation. The spatial profiles across the deformation show that the subsidence follows a "v" type pattern.

The results obtained from the proposed method were compared to the levelling data collected by NCC in two periods, 2004 and 2005 (Arabi et al. 2008). The available levelling data consists of five levelling tracks, SB1, SB2, SB3, SB4 and HQH as illustrated in Fig. 1 in different colours. The deformation rates at levelling stations are estimated from the trained neural network and then compared

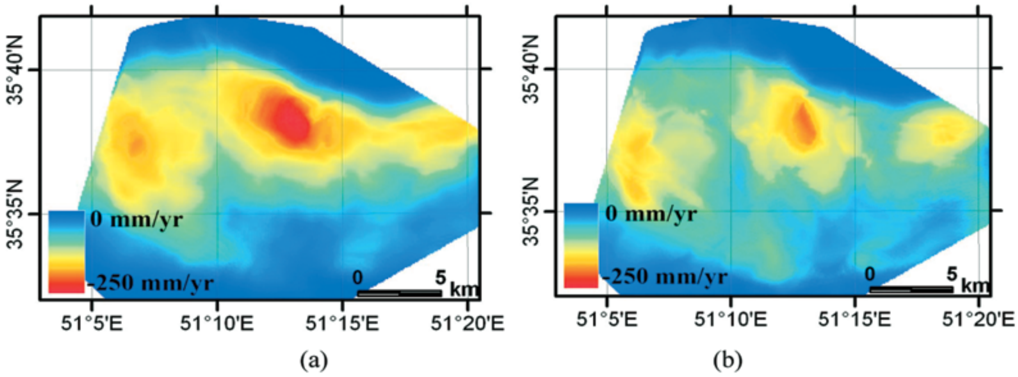

Fig. 7: Subsidence rate simulated from the proposed method applied on (a) descending dataset and (b) ascending dataset.

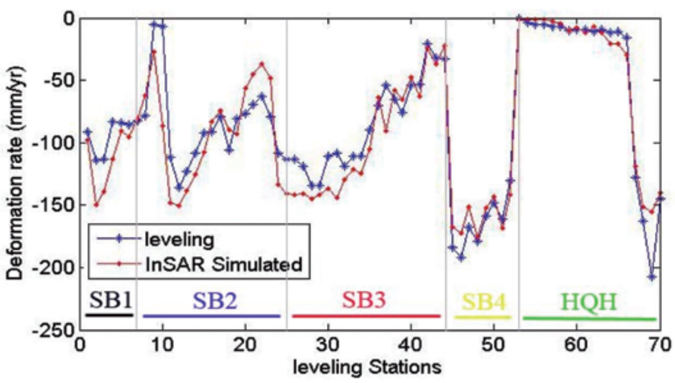

Fig. 8: Comparison of subsidence rate inferred from the proposed method (red lines) and levelling (blue lines) across different levelling tracks SB1, SB2, SB3, SB4 and HQH.

to the values measured by levelling. The comparison between levelling measurements and the vertically-converted subsidence rate estimated from the proposed method is shown in Fig. 8. The overall RMSE between levelling measurements and the vertically-converted subsidence rate extracted from the proposed method is estimated as 19.8 mm/a.

The different deformation rate of both datasets is most likely due to the different time intervals covered by the radar data (2004 and 2008) and levelling measurements (2004 and 2005), though the spatial distribution of the rates from levelling is consistent with that derived from the proposed method.

According to the diagram of Fig. 3, in order to study the effect of each input variables on the subsidence the sensitivity analysis is performed at the end of each run for all pixels. In each run, the sensitivity of the subsidence to different input variables (7 factors in here) is calculated for each pixel using the updated weights (2). The calculated sensitivities are then sorted based on their values indicating the significance order of the input variables affected by the subsidence rate. The maximum value is corresponding to the most effective factor. Finally, the sensitivity analysis outcomes of all 50 runs are integrated to obtain more reliable results. The final result is presented as a histogram showing the number of pixels for which one factor is indicated as the most effective one (Fig. 9). For example, according to Fig. 9 in about 3500 pixels the most effective factor on the subsidence occurrence is the hydraulic conductivity (#1). In fact, the effectiveness of a factor is determined by the number of pixels in which that factor is the most effective one. According to Figs. 9a and 9b, the subsidence has the most sensitivity to the hydraulic conductivity, thickness of fine-grained sediments and water level decline.

A considerable fact is that the sensitivity analysis results separately obtained from the descending and ascending data are highly comparable. The significance orders extracted from both datasets are exactly similar. This may indicate the correctness of the generated model.

4 Conclusions

Studying the land subsidence first requires measuring the magnitude of the deformation caused by this phenomenon. Analysis of the temporal and spatial behaviour of the deformation caused by subsidence allows us to mitigate its devastating effects and manage water resources. PS-InSAR is a method recently developed to measure the deformation in an area suffering from temporal and spatial

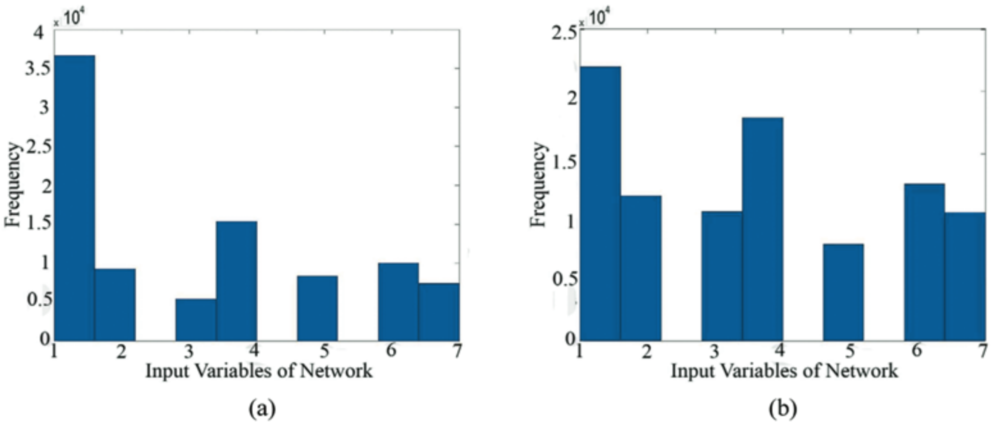

Fig. 9: Histograms of the sensitivity analysis results obtained from (a) descending data and (b) ascending data. The X-axis indicates the input variables (#1: hydraulic conductivity, #2: storage coefficient, #3: frequency of fine-grained sediments, #4: thickness of fine-grained sediments, #5: groundwater depth, #6: amount of water level decline and #7: alluvial thickness). Y-axis represents for the number of pixels.

decorrelation. However, this technique is able to measure the deformation at only PS pixels, the backscattering of which varies little in time. The subsidence estimation from PS-InSAR does not show local variations when the spatial density measurement points decreases which is mostly the case due to the occurrence of the subsidence in the rural areas. It is, on the other hand, critical to know about the local variations of the deformation particularly for the construction purposes. In this paper we presented an algorithm based on a neural network to estimate the subsidence rate in the non-PS pixels in which we were not able to directly measure the deformation by PS-InSAR method. Hydrogeology properties of the aquifer system were used as input variables of the network while the subsidence rate is taken as the network output. The PS pixels for which the subsidence rate is known from the PS-InSAR measurements were used to train and validate the network. The trained network was then applied to simulate the subsidence rate at all pixels (PS and non-PS pixels). This leads to retrieve the subsidence spatial pattern in the Tehran basin. The coincidence of the spatial pattern of the subsidence area with the cultivated area indicates that the subsidence in Tehran basin is due to groundwater exploitation. The maximum deformation rates estimated from descending and ascending datasets are 241 mm/a and 203 mm/a, respectively. The spatial profiles across the deformation area indicate that the subsidence follows a "v" type pattern. The results were then compared to the levelling measurements. The comparison showed that the deformation rates predicted at the levelling stations broadly agrees with the levelling measurements. The RMSE of 19.8 mm/a is most likely due to the different time intervals covered by the radar data (2004 and 2008) and levelling measurements (2004 and 2005), though the spatial distribution of the rates from levelling is consistent with that derived from the proposed method.

The sensitivity of the subsidence to different input parameters was finally investigated using the updated weights obtained in the training process. We found that the Tehran subsidence is mostly sensitive to the hydraulic conductivity, thickness of fine-grained sediments and water level decline.

Acknowledgements

We wish to thank the European Space Agency (ESA) for providing ENVISAT ASAR data. We convey our sincere gratitude to the Geological Survey of Iran for providing the hydrogeological information. The authors wish to thank the Delft University of Technology for all their kind scientific supports for persistent scatterer interferometry.

References

Amelung, F., Galloway, D.L., Bell, J.W., Zebker, H.A. & Laczniak, R.L., 1999: Sensing the ups and downs of Las Vegas – InSAR reveals structural control of land subsidence and aquifer-system deformation. – Geology **27** (6): 483–486.

Arabi, S., Maleki, E. & Talebi, A. 2008: Report of land subsidence in south-west of Tehran. – National Cartographic Center of Iran, national scientific report.

Crosetto, M., Tscherning, C.C., Crippa, B. & Castillo, M., 2002: Subsidence monitoring using SAR interferometry: reduction of the atmospheric effects using stochastic filtering. – Geophysical Research Letters **29** (9): 26.1–26.4.

Dehghani, M., Hooper, A., Hanssen, R., Valadan Zoej, M.J., Saatchi, S. & Entezam, I., 2009: Hybrid conventional and Persistent Scatterers SAR Interferometry for Land Subsidence Monitoring in southwest Tehran, Iran. – Fringe Workshop 2009, Italy.

Dehghani, M., Valadan Zouj, M.J., Entezam, I., Saatchi, S. & Shemshaki, A., 2010: Interferometric Measurements of Ground Surface Subsidence induced by Overexploitation of Groundwater. – Journal of Applied Remote Sensing **37** (1): 147–156.

Ferretti, A., Prati, C. & Rocca, F., 2000: Nonlinear subsidence rate estimation using Permanent Scatterers in Differential SAR Interferometry. – IEEE Transactions on Geoscience & Remote Sensing **38** (5): 2202–2212.

Fruneau, B. & Sarti, F., 2000: Detection of ground subsidence in the city of Paris using radar interferometry: isolation from atmospheric artifacts using correlation. – Geophysical Research Letters **27** (24): 3981–3984.

Galloway, D.L., Hudnut, K.W., Ingebritsen, S.E., Phillips, S.P., Peltzer, G., Rogez, F. & Rosen, P.A., 1998: Detection of aquifer system compaction and land subsidence using interferometric synthetic aperture radar, Antelope Valley, Mojave Desert, California. – Water Resources Research **34** (10): 2573–2585.

Galloway, D.L. & Hoffmann, J., 2007: The application of satellite differential SAR interferometry-derived ground displacements in hydrogeology. – Hydrogeology Journal **15:** 133–154.

González, P.J. & Fernández, I., 2011: Drought-driven transient aquifer compaction imaged using multitemporal satellite radar interferometry. – Geology **39:** 551–554.

Hashem, S., 1992: Sensitivity analysis for feedforward Artificial Neural Networks with differentiable activation functions. – 1992 International Joint Conferences on Neural Networks, IEEE Press **1:** 419–424, Baltimore, MD, USA.

Haykin, S.S., Haykin, S. & Van Veen, B., 1995: Neural Network: a Comprehensive Foundation, IEEE Version.

Hoffmann, J., Leake, S.A., Galloway, D.L. & Wilson, A.M., 2003: MODFLOW-2000 groundwater model – user guide to the subsidence and aquifer-system compaction (SUB) package. – U.S. Geological Survey Open-File Report **03-233**.

Hooper, A., Zebker, H., Segall, P. & Kampes, B., 2004: A new method for measuring deformation on volcanoes and other natural terrains using InSAR persistent scatterers. – Geophysical Research Letters **31:** 611–615.

Kampes, B.M., 2005: Displacements Parameter Estimation using Permanent Scatterer Interferometry. – Ph.D. thesis, Delft University of Technology.

Motagh, M., Djamour, Y., Walter, T.R., Wetzel, H.U., Zschau, J. & Arabi, S., 2006: Land subsidence in Mashhad Valley, northeast Iran: results from InSAR, levelling and GPS. – Geophysical Journal International **168**, doi: 10.1111/j.1365–246X.2006.03246.x.

Peltzer, G., Rosen, P., Rogez, F. & Hudnut, K., 1998: Poro-elastic rebound along the Landers 1992 earthquake surface rupture. – Journal of Geophysical Research **103:** 30.131–30.145.

Samieie-Esfahany, S., Hanssen, R.F., Thienen-Visser, K.V. & Muntendam-Bos, A., 2009: On the Effect of horizontal Deformation on InSAR Subsidence Estimates. – Fringe Workshop 2009, Italy.

Shemshaki, A., Blourchi, M.J. & Ansari, F.M., 2005: Earth subsidence review at Tehran plain-Shahriar (first report). – Report No: Engeo84-06/02, http://gsi.ir/General/Lang_en/Page_27/GroupId_01-01/TypeId_All/Start_20/Action_ListView/WebsiteId_13/3.html (30.10.2012).

Tesauro, M., Beradino, P., Lanari, R., SansoSti, E., Fornaro, G. & Franceschetti, G., 2000: Urban subsidence inside the City of Napoli (Italy) observed with synthetic aperture radar interferometry at Campi Flegrei caldera. – Journal of Geophysical Research **27:** 1961–1964.

Addresses of the authors:

Dr. Maryam Dehghani, Assistant Professor, Dept. of Civil and Environmental Engineering, School of Engineering, Shiraz University, Zand St., Shiraz, Iran, Tel.: +98-711-6133162, Fax: +98-711-6473161, e-mail: dehghani_rsgsi@yahoo.com

Dr. Mohammad Javad Valadan Zoej, Associate Professor, Faculty of Geodesy and Geomatics Engineering, K. N. Toosi University of Technology, Tehran, Iran, Tel.: +98-21-88770218, e-mail: valadanzouj@kntu.ac.ir.

Dr. Iman Entezam, Engineering Geology Group, Geological Survey of Iran (GSI), Tehran, Iran, Tel.: +98-21-64592228, e-mail: dr.entezam@gmail.com

Manuskript eingereicht: Mai 2012
Angenommen: September 2012